

## Molecular Mechanism of Activation of Class IA Phosphoinositide 3-Kinases (PI3Ks) by Membrane-Localized HRas

Braden D. Siempelkamp<sup>1</sup>, Manoj K. Rathinaswamy<sup>1</sup>, Meredith L. Jenkins<sup>1</sup>, and John E. Burke<sup>1,2</sup>

<sup>1</sup>From the Department of Biochemistry and Microbiology, University of Victoria, Victoria, British Columbia, Canada V8W 2Y2

Running title: *Molecular mechanism of the HRas-PI3K interaction*

<sup>2</sup>To whom correspondence should be addressed: John E. Burke, Department of Biochemistry and Microbiology, University of Victoria, Victoria, British Columbia, Tel: 1-250-721-8732, email: [jeburke@uvic.ca](mailto:jeburke@uvic.ca)

**Keywords:** Ras, HRas, phosphoinositide 3-kinase, PIK3CA, PIK3CD, lipid signaling, PI3K-Akt, HDX-MS, protein dynamics, hydrogen exchange, phosphoinositides

### ABSTRACT

Class IA PI3Ks are involved in the generation of the key lipid signaling molecule phosphatidylinositol 3,4,5-trisphosphate (PIP<sub>3</sub>), and inappropriate activation of this pathway is implicated in a multitude of human diseases, including cancer, inflammation, and primary immunodeficiencies. Class IA PI3Ks are activated downstream of the Ras superfamily of GTPases, and Ras-PI3K interaction plays a key role in promoting tumor formation and maintenance in Ras-driven tumors. Investigating the detailed molecular events in the Ras-PI3K interaction has been challenging because it occurs on a membrane surface. Here, using maleimide-functionalized lipid vesicles, we successfully generated membrane-resident HRas and evaluated its effect on PI3K signaling in lipid kinase assays and through analysis with hydrogen-deuterium exchange mass spectrometry (HDX-MS). We screened all class IA PI3K isoforms and found that HRas activates both p110 $\alpha$  and p110 $\delta$  isoforms, but does not activate p110 $\beta$ . The p110 $\alpha$  and p110 $\delta$  activation by Ras was synergistic with activation by a soluble phosphopeptide derived from receptor tyrosine kinases. HDX-MS revealed that membrane-resident HRas, but not soluble HRas, enhances conformational changes associated with membrane binding by increasing membrane recruitment of both p110 $\alpha$  and p110 $\delta$ . Together, these results afford detailed molecular insight into the Ras-PI3K signaling complex, provide a

framework for screening Ras inhibitors, and shed light on isoform specificity of Ras-PI3K interactions in a native membrane context.

### INTRODUCTION

The generation of membrane-resident lipid signals are a key component of signalling downstream of cell surface receptors. Some of the most important lipid signalling molecules are lipid phosphoinositides (1), in particular the species phosphatidylinositol 3,4,5 trisphosphate (PIP<sub>3</sub>), generated by the phosphoinositide 3-kinase (PI3K) family of enzymes, specifically the class I PI3Ks. PIP<sub>3</sub> acts as a key recruitment signal for enzymes containing PIP<sub>3</sub>-binding domains, and the recruitment of these enzymes mediate many key cellular functions, including growth, motility, and survival (2). Due to the critical importance of PIP<sub>3</sub> as a growth regulator, the activation of PI3Ks must be tightly controlled. They are able to be activated downstream of a number of plasma membrane associated signalling complexes including receptor tyrosine kinases (RTKs), G-protein coupled receptors, and the Ras superfamily of GTPases (3-5).

Understanding the regulation of PI3Ks are of fundamental importance as they are frequently involved in many human diseases, including cancer (6) and primary immune deficiencies (7). The upstream activators of PI3Ks are also frequently misregulated in cancer, with the K<sub>Ras</sub> isoform of Ras being the most frequently mutated

oncogene in all of human cancer (8, 9). Understanding the molecular basis for how upstream stimuli activate PI3K is of fundamental importance in designing novel therapeutic strategies to target PI3K signalling in disease.

The class I PI3Ks are further split into two subgroups, class IA and IB, dependent on the presence of different regulatory subunits. The class IA PI3Ks are obligate heterodimers composed of a p110 catalytic subunit (p110 $\alpha$ , p110 $\beta$ , p110 $\delta$ ) with a p85 regulatory subunit (p85 $\alpha$ , p55 $\alpha$ , p50 $\alpha$ , p85 $\beta$ , p55 $\gamma$ ) (10). Both p110 and p85 subunits are large multi domain proteins (Fig. 1A), with the p110 composed of an adaptor binding domain (ABD) that mediates tight binding to p85, a Ras-binding domain (RBD) that mediates interaction with Ras superfamily members, a C2 domain that forms an inhibitory contact with p85 and mediates membrane binding, a helical scaffolding domain that forms inhibitory contacts with p85, and a kinase domain that phosphorylates phosphatidylinositol 4,5 bisphosphate (PIP<sub>2</sub>) to generate PIP<sub>3</sub>. The p85 regulatory subunit is composed of two SH2 domains (nSH2 and cSH2) linked by a coiled-coil inter-SH2 (iSH2) domain, which participate in multiple inhibitory interactions with the p110 subunit. The p85 regulatory subunit plays three key roles for class I PI3Ks: they stabilize the catalytic subunit, inhibit enzyme activity, and allow for activation downstream of phosphorylated receptors (such as receptor tyrosine kinases) through engagement of the SH2 domains.

The different class IA PI3K isoforms vary greatly in their ability to be activated downstream of various stimuli. The p110 $\alpha$  isoform is able to be activated downstream of phosphorylated receptors and Ras, and plays a fundamental role in propagating signals downstream of insulin signalling (11). The p110 $\beta$  isoform is also able to be activated downstream of phosphorylated receptors, however, it is not activated downstream of Ras, but instead is activated downstream of Rho family GTPases (12), as well as G-beta-gamma subunits derived from G-protein coupled receptors (13, 14). The p110 $\delta$  subunit, which is primarily expressed in immune cells, can also be activated downstream of phosphorylated receptors, and has been proposed to be activated downstream of a subset of Ras isoforms, with the RRas2 isoform

TC21 being implicated in its activation in T-cells (15).

The structure of the class IB p110 $\gamma$  isoform of PI3K has been solved in complex with the active GMPPNP-bound state of HRas (16). This structure has played an important role in understanding PI3K activation, and allowed for the generation of RBD mutant PI3Ks that are deficient in Ras binding. This has played a fundamental role in elucidating the role of the PI3K-Ras interaction in many signalling pathways and disease states (12, 17-19), and revealed the key role of the p110 $\alpha$ -Ras interaction in promoting tumor formation, angiogenesis, and tumor survival in Ras-driven cancers (17-19). However, a major limitation in understanding the full molecular details of the PI3K-Ras interaction is that Ras is membrane resident due to multiple lipidation sites, and this has made native Ras-effector interactions exceedingly challenging to study. Recent NMR studies examining KRas on membranes revealed unexpected membrane-bound conformations of KRas (20), and this highlights the importance of examining the PI3K-Ras interaction in its native membrane-bound conformation.

To fully explore the interaction of the class IA PI3Ks with Ras in a biologically relevant context, we have successfully generated covalently-linked membrane resident HRas using a previously described maleimide labeled lipid strategy (20-22). Membrane-coupled HRas was used to probe the activation of all of the class IA PI3Ks in the presence and absence of a phosphopeptide mimicking RTK activation. To fully characterize the molecular details of the PI3K-Ras interaction we used hydrogen deuterium exchange mass spectrometry (HDX-MS) to probe the dynamics of this interaction on a membrane surface. We surprisingly found a considerable synergy between RTK and Ras activation, as well as unexpected isoform specific differences in activation downstream of HRas. HDX-MS revealed a number of conformational changes upon Ras binding, and provides the most detailed molecular insight into the interaction of Ras with the full-length p110/p85 complex.

## RESULTS

### *Biochemical reconstitution of HRas on a membrane*

In order to accurately examine the native HRas-PI3K interaction, HRas was reconstituted on vesicles with a composition roughly mimicking the plasma membrane (5% PIP<sub>2</sub>, 10% PE-MCC, 15% PC, 30% PS, and 40%PE). This composition of lipids was used as we have previously optimized membrane composition for enhanced PI3K-membrane binding {Dornan:2017hu, Burke:2012dh, Burke:2011jz}. This membrane composition was used for all further biochemical experiments. *In vivo*, HRas undergoes differential lipidation on three terminal cysteine residues, C181, C184, and C186 (Fig. 1). We chose to use the HRas G12V C118S 1-181 construct (referred to as HRas hereafter). The HRas C118S 1-181 construct has been previously used in maleimide conjugation reactions and has been shown to have biochemical and structural properties indistinguishable from wild-type lipidated HRas (22-24). This construct ends in a C-terminal cysteine, C181, which is lipidated in cells and allows for its integration into the plasma membrane. In the presence of maleimide, the terminal cysteine (C181) participates in the thiol-conjugation reaction to form a stable thioether bond with maleimide-functionalized lipid vesicles, effectively mimicking the membrane-bound state (Fig. 1). The purified HRas contained a G12V mutation, an oncogenic mutation that prevents GAP-induced GTPase activity (9). Any remaining uncoupled soluble HRas was separated from HRas-coupled vesicles by size-exclusion chromatography (Fig. 1). HRas coupling efficiencies varied but were in the range of 5-10% of total lipid maleimide.

#### *HRas-mediated activation of PI3Ks is dependent on HRas membrane association*

To test whether HRas membrane association was required for successful activation of PI3Ks, lipid kinase assays measuring the production of ADP were used to assay PI3K activities in the presence of soluble (non-coupled) HRas G12V C118S 1-181 (sHRas). All assays were carried out with soluble HRas loaded with GTP $\gamma$ S at a final concentration of 5  $\mu$ M. Both p110 $\alpha$ /p85 $\alpha$  and p110 $\delta$ /p85 $\alpha$  were not activated by sHRas in both the presence and absence of a stimulating RTK-derived phosphopeptide (PDGFR residues 735–767, with pY740 and pY751, referred to as pY)(Fig. 2). Surprisingly

there was even a small decrease in p110 $\alpha$ /p85 $\alpha$  lipid kinase activity in the presence of soluble HRas. This emphasized the necessity of HRas membrane-localization to successfully study HRas-PI3K interactions.

#### *HRas-coupled vesicles potently activate PI3K $\alpha$ and PI3K $\delta$ but not PI3K $\beta$*

All class IA PI3Ks were assayed for their lipid kinase activities both with and without vesicle-bound HRas and in the presence and absence of RTK derived phosphopeptide, which allowed for the examination of multiple PI3K activation states. All of the class IA catalytic isoforms were screened in complex with the full-length p85 $\alpha$  regulatory subunit. The different complexes of p110 $\alpha$ /p85 $\alpha$ , p110 $\beta$ /p85 $\alpha$ , and p110 $\delta$ /p85 $\alpha$  will be referred to as PI3K $\alpha$ , PI3K $\beta$ , and PI3K $\delta$ , respectively, throughout the rest of the text. Activation of PI3Ks was dependent on the bound-nucleotide state of HRas. Membrane-resident HRas potently activated PI3K activity when bound to GTP $\gamma$ S (Fig. 3B), with only a very minor increase in PI3K activity when HRas was bound to GDP. This result confirmed that the HRas-mediated PI3K activation is regulated via the prototypical GTPase cycle (*i.e.* GTP-bound = active; GDP-bound = inactive), as expected.

The lipid kinase activities of both PI3K $\alpha$  and PI3K $\delta$  were only partially increased by membrane-resident HRas alone. For PI3K $\alpha$ , membrane-resident HRas led to a ~2.5 fold increase in activity, while in PI3K $\delta$  this activation was ~2 fold. The presence of phosphopeptide resulted in a massive synergistic increase in lipid kinase activity for both enzymes. PI3K $\alpha$  and PI3K $\delta$  were activated ~11 fold and ~30 fold, respectively, by membrane-resident HRas relative to phosphopeptide alone. The synergy between HRas and RTK-derived phosphopeptides is consistent with previous results for p110 $\alpha$  using lipidated HRas (25). The activation of PI3K $\delta$  by HRas was intriguing, as previous studies have suggested that HRas does not activate PI3K $\delta$  (26). Recent analysis examining the ability of each Ras isoform to interact with all of the class IA PI3Ks indicated that soluble active HRas can pulldown PI3K $\delta$  (12). Our results indicate that PI3K $\delta$  is fully competent to be activated by HRas, and that both PI3K $\alpha$  and PI3K $\delta$  are synergistically

activated by both membrane-resident HRas and phosphorylated receptors and their adaptors.

PI3K $\beta$  was not significantly activated by membrane-resident HRas in both basal and pY-stimulated states. These results are in agreement with studies showing that PI3K $\beta$  does not interact with Ras subfamily GTPases, such as HRas, but instead is activated by the Rho subfamily GTPases Cdc42 and Rac1(12).

#### *HDX-MS reveals the molecular mechanism of the HRas-PI3K interaction*

To further understand the molecular details of membrane-resident HRas activation of both PI3K $\alpha$  and PI3K $\delta$ , and answer why membrane localized HRas leads to a large increase in lipid kinase activity, we used hydrogen deuterium exchange mass spectrometry (HDX-MS). HDX-MS is a powerful analytical method that measures the exchange rate of amide hydrogens with deuterated buffer. As the main determinant of amide exchange is their involvement in secondary structure, their rate of exchange acts as an excellent probe of protein dynamics. The technique is particularly useful in analyzing the interaction of peripheral membrane proteins with membranes and membrane-localized proteins (27-32).

We carried out HDX-MS experiments on pY-activated p110 $\alpha$ /p85 $\alpha$  and p110 $\delta$ /p85 $\alpha$  complexes under four conditions: (i) alone, and in the presence of (ii) plasma membrane mimic vesicles, (iii) soluble HRas, or (iv) HRas-coupled plasma membrane mimic vesicles. Experiments were also carried out in the absence of pY in the presence of membrane and HRas-coupled membranes. Membrane was present at 0.2 mg/ml, soluble HRas was present at 3  $\mu$ M, coupled HRas was present at 327 nM, PI3K was present at 200 nM, and soluble RTK-derived pY was present at 5  $\mu$ M. D<sub>2</sub>O was added and exchange was quenched at three time points (3s, 30s and 300s). For experiments performed in the absence of pY the coupled HRas concentration was increased to  $\sim$ 1  $\mu$ M and the exchange was quenched at 3s and 300s. All experiments were carried out in triplicate. Deuterium localization was carried out by pepsin digestion, and the analyzed list of peptic peptides contains 137 peptides for p110 $\delta$  (covering 90% of the protein sequence), 147 peptides for p110 $\alpha$  (covering 85.5% of the protein

sequence) and 84 peptides for p85 $\alpha$  (covering 88% of the protein sequence). The full set of peptides and their levels of deuterium incorporation are shown in SI Figures S1-S6. Peptides that showed differences in amide exchange greater than 0.4 Da and 5% at any time point of exchange, as well as having t-test values of  $p < 0.05$  between conditions were considered significant.

#### *HDX-MS of PI3K $\alpha$ :*

Comparing membrane-bound PI3K $\alpha$  to PI3K $\alpha$  bound to HRas-coupled membranes in the presence of pY revealed changes in exchange consistent with both enhanced membrane binding as well as interaction with HRas (Fig. 4, S7). In p110 $\alpha$ , the presence of vesicle-coupled HRas, but not soluble HRas, resulted in decreased H/D exchange in several regions of the RBD. No significant decreases in exchange in PI3K $\alpha$  were seen in the presence of soluble HRas, despite being present at  $>10$  fold excess concentration over PI3K (Fig. S7). A large decrease with membrane-bound HRas was observed in peptides containing the conserved T208 (192-209). This residue aligns with the essential T232 in PI3K $\gamma$  which has been shown to form hydrogen bonds with E37 in HRas (16). Another region that showed decreases in exchange in the RBD (223-233) contains the conserved K227, which aligns with K251 in PI3K $\gamma$ . K251 forms salt bridges with D33 and D38 in HRas and is also required for HRas binding.

Membrane-coupled HRas also caused decreased exchange in numerous regions that had been previously identified as membrane-binding regions. These include residues spanning the loop between helices  $\alpha$ 1k and  $\alpha$ 2k to the loop between  $\alpha$ 2k and  $\alpha$ 3k in the N-lobe of kinase domain (716-743). This region constitutes a putative membrane binding region (33) with multiple basic residues (K720, K723, K724, K729, K733, R740 and R741). Decreases were also seen in the C-terminus, with  $>20\%$  decreases in the disordered region from 1060-1068, and smaller decreases ( $<10\%$ ) in the latter half of the  $\alpha$ 11k helix at the end of the regulatory arch (1039-1058). The N-lobe (720-734) and C-terminus showed very little protection from H/D exchange in the condition with PI3K alone, with a large decrease in these regions at early time points in the presence of



HRas coupled membranes. This is indicative of either formation of secondary structure or stabilization of very transient secondary structure upon membrane interaction.

Consistent with data previously published (29), the ABD-RBD linker (100-119) and the ABD-kinase domain interface (71-76) showed increased exchange upon membrane binding, and HRas-coupled membranes led to further increases in this region. This is consistent with a reorientation of the ABD relative to the kinase domain upon membrane binding. Increases in exchange were also seen at the interface of the C2 domain of p110 $\alpha$  (444-456) and the iSH2 domain of p85 $\alpha$  (470-476, 556-570) with HRas-coupled vesicles. Interestingly, a region of the nSH2 (405-420) showed decreased exchange upon membrane binding, with HRas-coupled vesicles enhancing this difference. These decreases in exchange may be due to the putative role of nSH2 as a membrane-binding domain (34). For most of these regions, very small changes were seen when comparing PI3K in solution to PI3K with membranes, while membrane-coupled HRas caused larger changes in these regions suggesting that HRas is enhancing membrane binding.

Experiments carried out in the absence of pY comparing HRas coupled membranes and membranes alone revealed very small changes in exchange in some of the same regions (p110 $\alpha$  region 100-119 and p85 $\alpha$  regions 457-466, and 556-581, Fig. S7). However, there were no changes in putative membrane binding regions, consistent with the kinase assay data suggesting that pY is required for full HRas driven activation.

#### *HDX-MS of PI3K $\delta$ :*

Analogous to PI3K $\alpha$ , very similar regions in the PI3K $\delta$  complex exhibited large differences in exchange with HRas-coupled vesicles (Fig. 5, S8). The changes in HDX in the presence of membrane were consistent with data previously published (32, 35). The presence of membrane-coupled HRas led to decreases in the p110 $\delta$  RBD, and the largest decrease was seen in peptides containing the conserved K223 (221-238). A large decrease was also observed in residues upstream of the conserved T204 (192-202). Similar to p110 $\alpha$ , these regions did not exhibit significant protection in the presence of soluble HRas.

As for p110 $\alpha$ , previously annotated membrane-binding areas showed enhanced differences in exchange with membrane-coupled HRas, suggesting that for both p110 $\alpha$  and p110 $\delta$  HRas strengthens membrane interactions. As in p110 $\alpha$ , a part of  $\kappa\alpha 11$  and the disordered C-terminus region (1023-1033) showed improved protection with HRas-coupled vesicles relative to membrane. HRas-coupled vesicles also resulted in tighter membrane interaction at the activation loop (927-935) and a proposed membrane-binding site (850-856) spanning the  $\kappa\alpha 4$ - $\kappa\alpha 5$  loop and  $\kappa\alpha 5$  in the C-lobe (35). Among the regions in p110 $\delta$  that showed increased exchange with membrane, HRas-coupled vesicles caused enhanced exposure at the ABD-kinase interface (71-82). In p85 $\alpha$ , HRas-coupled vesicles resulted in exposure of the iSH2-C2 interface (470-476, 556-570) and a significant protection of the nSH2 (405-420).

Experiments carried out in the absence of pY comparing HRas coupled membranes and membranes alone revealed very small changes in exchange in some of the same regions (p110 $\delta$  RBD region 192-201, 228-238, Fig. S8). However, there were no changes in putative membrane binding regions, or conformational changes in p85 $\alpha$ . This is consistent with the kinase assay data suggesting that membrane coupled HRas alone has little effect on p110 $\delta$  activation, with pY required for full HRas driven activation.

In summary, membrane-coupled HRas primarily enhanced the increases or decreases in H/D exchange that were observed in RTK activated PI3K $\alpha$  and PI3K $\delta$  with membranes alone. These changes suggest that HRas-coupled vesicles greatly improve the residence time of PI3Ks on membranes, and reinforce their interaction with their lipid substrate. Soluble HRas, on the other hand, neither interacted stably nor caused significant conformational changes, thereby explaining its inability to activate these enzymes.

## DISCUSSION

The class IA PI3Ks are essential enzymes in propagating numerous cellular signals that promote growth, development, and survival. Their misregulation plays a key role in many diseases, and fully understanding the molecular mechanism by which they are activated is essential to reveal

novel routes to therapeutic intervention in PI3K-mediated diseases. One of the most important upstream activators of the class I PI3Ks are the Ras superfamily of GTPases. This interaction is particularly important in cancer development and progression in many tumor types. The KRas isoform is the most frequently mutated oncogene in all of human cancer (8), with the *PIK3CA* gene encoding p110 $\alpha$  also frequently mutated in many human cancers (6). The generation of point mutants in the RBD of *PIK3CA* that are deficient in activation downstream of Ras revealed that the p110 $\alpha$ -Ras interaction is essential for tumorigenesis (17), angiogenesis (18), and tumor maintenance (19). The RBD mutant of *PIK3CB* encoding p110 $\beta$  revealed that interaction with Rho family GTPases plays key roles in cell migration, and led to protection in mouse models of lung fibrosis (12).

The structure of PI3K $\gamma$  bound to HRas allowed for the determination of the molecular basis for the interaction of Ras (16), however, many important aspects of Ras activation of PI3K on membranes have remained unclear. To fully examine the activation of class IA PI3Ks by Ras, we have generated Ras-coupled membranes mimicking the plasma membrane, and this has allowed us to examine the Ras-PI3K interaction in a native membrane context. We find that active GTP $\gamma$ S-loaded soluble HRas has no effect on lipid kinase activity for all class IA PI3K isoforms, consistent with previous reports for p110 $\gamma$  (36). When HRas is presented in the context of being coupled to lipid membranes there is an increase in lipid kinase activity for both p110 $\alpha$  and p110 $\delta$ , with the lack of activation of p110 $\beta$  consistent with previous reports that p110 $\beta$  is only activated downstream of Rho family GTPases (12). The activation downstream of Ras was greatly increased if there was co-activation by phosphopeptides mimicking activation downstream of receptor tyrosine kinases. Thus, *in vitro* both p110 $\alpha$  and p110 $\delta$  require both Ras and RTK inputs for full activation, with both Ras proteins and phosphorylated RTKs promoting the formation of partially active PI3K states (Fig. 6). The robust activation of PI3K $\delta$  by HRas-coupled vesicles was unexpected, as previous reports in HEK293T cells had suggested that HRas does not lead to activation of p110 $\delta$  (26). What our experiments reveal is that the p110 $\delta$  isoform can

be robustly activated by membrane-localized HRas, and that p110 $\delta$  activation in cells may require the cooperation of other synergistic upstream activating inputs in addition to HRas.

The previously most detailed analysis of the Ras superfamily of GTPases and their interaction with different PI3K isoforms was carried out through generation of recombinant soluble Ras isoforms and their ability to pull down different class I PI3Ks (12). The differences in H/D exchange seen with soluble and membrane-coupled HRas revealed disparities in the ability of soluble HRas and membrane coupled HRas to interact with PI3Ks. This underscores the key role of the membrane in promoting the interaction between PI3Ks and Ras, and full analysis of how different PI3K isoforms interact with different Ras isoforms will require examination in a native membrane environment.

To examine the molecular mechanism of how HRas mediated PI3K activation on membranes, we used HDX-MS. For both p110 $\alpha$  and p110 $\delta$  we found that the presence of HRas led to protection of the RBD-Ras interface and an amplification of deuterium exchange changes that occur upon membrane binding. These changes include a reorientation of the ABD relative to the rest of the catalytic subunit, disruption of the C2-ISH2 interface, and interaction of the membrane binding regions of the kinase domain with membranes, as previously discovered for all of the class IA PI3Ks (13, 29, 32, 35). This suggests that the likely mechanism of activation by Ras is driven through enhanced membrane interaction. It has been previously suggested that a possible mechanism for PI3K activation could be driven through an allosteric conformational change induced by interactions between the kinase domain of p110 and Ras (16). No differences in H/D exchange were detected at this proposed interface for either soluble or membrane-coupled HRas, suggesting that this is unlikely to be the mechanism of activation. The very weak interaction of HRas with PI3K in solution compared to on membranes suggests that the membrane plays a key role in enhancing the local concentration of each component, and that this is likely to explain the enhanced PI3K-HRas interaction on membranes. Previous studies exploring the G $\beta\gamma$  activation of both p110 $\gamma$  and p110 $\beta$  revealed that interaction with membranes

caused allosteric conformational changes at the G $\beta\gamma$  interface (13, 37), implying that membrane played a key role in priming the interaction between these two proteins. No similar membrane-induced conformational changes are seen in the HRas-PI3K interface, indicating a key difference between these two protein-membrane PI3K complexes.

Both PI3Ks and Ras are key molecular targets for the development of novel therapeutic small molecule inhibitors. Fully understanding the complement of how different Ras isoforms activate different PI3K isoforms in a native biological context will be beneficial in understanding their role in different signalling processes and disease states. Our work reveals that the generation of maleimide-coupled Ras isoforms on plasma membrane mimic vesicles is a useful tool to rapidly screen different Ras isoforms for their ability to activate different class I PI3K isoforms. Non-covalent Ras inhibitors have recently been reported that are non-selective in their ability to differentiate between GTP- and GDP-loaded forms (38). The use of membrane-coupled Ras in PI3K activity assays could play a key role in rapid screening of these inhibitors for their ability to disrupt PI3K-Ras interactions. Altogether our results reveal the most detailed molecular understanding for how membrane-localized Ras is able to activate PI3Ks, and provides a useful platform for future screening of how different Ras isoforms activate different PI3K isoforms.

## EXPERIMENTAL PROCEDURES

### Plasmid Generation

Original plasmids of the wild-type HRas, p110 $\alpha$ , p110 $\beta$ , p110 $\delta$  and p85 $\alpha$  were a kind gift from the Williams laboratory at the MRC-LMB. HRas single substitution mutations were generated using site-directed mutagenesis according to published protocols and C-terminal residues were removed using Gibson assembly.

### Protein Expression and Purification

All PI3K complexes were similarly expressed as previously described (32). To express PI3K complexes, an optimised ratio of p110:p85 $\alpha$  baculovirus was used to co-infect *Spodoptera frugiperda* (Sf9) cells between  $1\text{--}2 \times 10^6$  cells/mL.

Co-infections were harvested between 40–72 hours and washed with ice-cold PBS before snap-freezing in liquid nitrogen. PI3K proteins were purified by lysing cells and performing sequential nickel affinity, streptavidin affinity, and size exclusion purifications. All steps in protein purification were carried out on ice, or in a 4 °C cold room. Frozen Sf9 pellets were re-suspended in lysis buffer (20 mM Tris pH 8.0, 100 mM NaCl, 10 mM imidazole pH 8.0, 5% glycerol (v/v), 2 mM  $\beta$ ME, protease inhibitor (Protease Inhibitor Cocktail Set III, Sigma)) and sonicated on ice for 1 minute (15s on, 15s off, level 4.0, Misonix sonicator 3000). Triton X-100 was added to the lysate at a concentration of 0.1% and centrifuged at 20,000 g for 45 minutes (Beckman Coulter Avanti J-25I, JA 25.50 rotor). The supernatant was loaded onto a 5 mL HisTrap™ FF column (GE Healthcare) equilibrated in NiNTA A buffer (20 mM Tris pH 8.0, 100 mM NaCl, 10 mM imidazole pH 8.0, 5% (v/v) glycerol, 2 mM  $\beta$ ME). The column was washed with 20 mL of NiNTA A buffer, 20 mL of 6% NiNTA B buffer (20 mM Tris pH 8.0, 100 mM NaCl, 200 mM imidazole pH 8.0, 5% (v/v) glycerol, 2 mM  $\beta$ ME) before being eluted with 100% NiNTA B. The elution was loaded onto a 1 mL StrepTrap™ HP column (GE Healthcare) equilibrated in Hep A buffer (20 mM Tris pH 8.0, 100 mM NaCl, 5% (v/v) glycerol, 2 mM  $\beta$ ME). To cleave the strep-tag, 1 mL of a TEV protease solution (~0.08 mg/mL) was loaded onto the column and incubated for 3 hours. Protein was eluted using 2 mL of Hep A buffer. The StrepTrap™ elution was concentrated in a 50,000 MWCO Amicon concentrator (Millipore). Concentrated proteins were injected onto a Superdex™ 200 10/300 GL Increase size-exclusion column (GE Healthcare) equilibrated in PI3K gel filtration buffer (20 mM HEPES pH 7.5, 150 mM NaCl, 0.5 mM tris(2-carboxyethyl)phosphine (TCEP)). Proteins were concentrated, frozen in liquid nitrogen at a concentration between 0.5–3 mg/mL, and was stored at -80 °C.

### Purification of HRas G12V C118S 1-181

HRas G12V C118S 1-181 was transformed into *Escherichia coli* (BL21 (DE3)). Bacterial cultures were induced with 1 mM IPTG after growth to an OD<sub>600</sub> of 0.6–0.9 in 2X YT broth containing ampicillin at 100  $\mu$ g/mL. Induction was

allowed to proceed for 4 hours at 37 °C. The bacteria were harvested by centrifugation and the pellets stored at -80 °C.

Frozen *E. coli* pellets were re-suspended in lysis buffer and sonicated on ice for 5 minutes (10 s on, 10 s off, level 6.0, Misonix sonicator 3000). Triton X-100 was added to the lysate at a concentration of 0.1% and centrifuged at 20 000 g for 45 minutes (Beckman Coulter Avanti J-25I, JA 25.50 rotor). The supernatant was then loaded onto a 5 mL HisTrap™ FF column (GE Healthcare) equilibrated in NiNTA A buffer. The column was washed with 20 mL of NiNTA A buffer, 20 mL of 6% NiNTA B buffer before being eluted with 100% NiNTA B. The elution was buffer exchanged with NiNTA A buffer in a 10 000 MWCO Amicon concentrator (Millipore). The sample was concentrated to 1-3 mL and TEV protease was added to a final concentration of ~0.3 mg/mL. The cleavage was allowed to proceed overnight at 4 °C. To de-enrich the TEV protease, the protein solution was loaded onto a HisTrap™ FF column and eluted with 10 mL of NiNTA A buffer. The elution was concentrated to ~2 mL.

Nucleotide (GDP or GTPγS) was added in two-fold molar excess relative to HRas along with 25 mM EDTA. After incubation for 1 h at room temperature, the solution was buffer exchanged with phosphatase buffer (32 mM Tris pH 8.0, 200 mM ammonium sulphate, 0.1 mM ZnCl<sub>2</sub>, 2 mM βME) and 1 unit of immobilized calf alkaline phosphatase (Sigma) was added per milligram of HRas along with a two-fold excess of nucleotide. After incubation for 1 h at room temperature, MgCl<sub>2</sub> was added to 30 mM to lock bound nucleotide in place and immobilized phosphatase beads were removed using a 0.22 micron spin filter (EMD Millipore).

The protein was buffer exchanged with Ras gel filtration buffer (20 mM HEPES pH 7.0, 150 mM NaCl, 1 mM MgCl<sub>2</sub>) and concentrated to less than 1 mL. Protein was injected onto a Superdex™ 75 10/300 GL size-exclusion column (GE Healthcare) equilibrated in Ras gel filtration buffer. Proteins were concentrated to greater than 5 mg/mL and used in subsequent maleimide-coupling experiments.

#### *Lipid Vesicle Preparation*

Plasma membrane mimic maleimide-functionalized vesicles (PM-MCC) were

composed of 5% porcine brain phosphatidylinositol 4,5-bisphosphate (PIP<sub>2</sub>), 10% maleimidomethyl phosphoethanolamine (PE-MCC), 30% bovine brain phosphatidylserine (PS), 40% egg yolk phosphatidylethanolamine (PE), and 15% egg yolk phosphatidylcholine (PC). Lipid components dissolved in organic solvent were combined and solvent was evaporated under a stream of N<sub>2</sub> gas. The lipid film was desiccated under vacuum for 60 minutes. Lipids were resuspended at 5 mg/mL in lipid buffer (25 mM HEPES pH 7.0, 100 mM NaCl, 10% glycerol) followed by sonication for 10 minutes. The vesicle solutions were subjected to three freeze-thaw cycles. Vesicles were extruded 11 times through a 100 nm filter using a LipX extruder (T&T Scientific). Vesicles were snap-frozen in liquid nitrogen and stored at -80°C.

#### *Maleimide Coupling*

HRas was added to 100 μL of 5 mg/mL PM-MCC vesicles at a molar ratio of 1.25 HRas per maleimide. The thiol-maleimide conjugation reaction was allowed to proceed under nitrogen for 90 minutes at room temperature, followed by incubation at 4 °C overnight. A vesicles-only control was treated identically to the HRas sample with the exception that buffer was added in place of HRas. Reactions were terminated via the addition of 5 mM βME. HRas-coupled and non-coupled vesicles were separated from soluble HRas by size-exclusion chromatography on a Superdex™ 200 Increase 5/150 GL column (GE Healthcare) equilibrated in Ras gel filtration buffer. Both HRas-coupled and non-coupled vesicles were diluted to a final concentration of 1.0 mg/mL. The coupled HRas concentration was determined via intensity interpolation (ImageJ) of an SDS-PAGE standard curve using known soluble HRas concentrations.

#### *Lipid Kinase Assays*

Lipid kinase assays monitoring hydrolysis of ATP were carried out using the Transcreener ADP<sup>2</sup> Fluorescence Intensity (FI) assay (Bellbrook labs). Lipid vesicles with or without coupled HRas were used at a final concentration of 0.45 mg/ml, with ATP present at 100 μM. Membrane coupled HRas was present at a final concentration of 1.3 μM. Protein solutions containing either pY (PDGFR residues 735–767, with pY740 and



pY751, referred to afterwards as pY; final concentration in assay 1  $\mu$ M) or blank solution in 2X PI3K kinase buffer (100 mM HEPES pH 7.5, 200 mM NaCl, 6 mM  $MgCl_2$ , 2 mM EDTA, 0.06% CHAPS, 2 mM TCEP) were equilibrated briefly at 23 °C. In the soluble HRas assays, soluble HRas or blank solution was incorporated into the 2X protein solution (final assay concentration 5  $\mu$ M). Kinase reactions were started by addition of 2  $\mu$ L of protein solution to 2  $\mu$ L of 2X substrate solution (0.9 mg/mL lipid vesicles  $\pm$  HRas, 200  $\mu$ M ATP) in a 384-well black microplate (Corning). The reaction was allowed to proceed at 23 °C for 60 minutes before the addition of 2X Stop and Detect buffer (1X Stop and Detect Buffer, 8 nM ADP Alexa594 Tracer, 93.7  $\mu$ g/mL ADP<sup>2</sup> Antibody-IRDye QC-1). Antibody, tracer, and ADP were equilibrated for 60 minutes. Fluorescence intensity was measured using a Cytation 5 plate reader with  $\lambda_{excitation}$  = 590 nm and  $\lambda_{emission}$  = 620 nm (20 nm bandwidth; Molecular Devices). Specific activity was calculated using an ATP/ADP standard curve according to the Transcreeper ADP FI protocol. Statistical analyses for differences in lipid kinase activity shown in figures were carried out using a paired student's t-test.

#### *Hydrogen Deuterium Exchange Mass Spectrometry (HDX-MS)*

HDX experiments were described similar to as described in (39). In brief, HDX experiments were conducted in 52.5  $\mu$ L reactions with a final concentration of 225 nM for PI3K $\alpha$  and 286 nM for PI3K $\delta$ . Three conditions were tested: PI3K in the presence of phosphopeptide (5  $\mu$ M pY) (i) alone and with (ii) soluble HRas (3  $\mu$ M), (iii) lipid vesicles (5% PIP<sub>2</sub>, 30% PS, 40% PE, 10% PE-CC (reduced), 15% PC) present at 100  $\mu$ g/mL (iv) HRas-coupled vesicles. Deuterium exchange was initiated by the addition of 40  $\mu$ L deuterated buffer (10 mM HEPES pH 7.5, 100 mM NaCl, 98% (v/v) D<sub>2</sub>O). Exchange was carried out for three time points (3 s, 30 s, and 300 s at 23 °C) and terminated by the addition of 21  $\mu$ L ice-cold quench buffer (2 M guanidine-HCl, 3% formic

acid). Samples were immediately frozen in liquid nitrogen and stored at -80 °C.

Protein samples were rapidly thawed and injected onto a UPLC system at 2 °C. Protein was run over two immobilized pepsin columns (Applied Biosystems; porosyme, 2-3131-00) at 10 °C and 2 °C at 200  $\mu$ L/min for 3 minutes, and peptides were collected onto a VanGuard precolumn trap (Waters). The trap was subsequently eluted in line with an Acquity 1.7  $\mu$ m particle, 100  $\times$  1 mm<sup>2</sup> C18 UPLC column (Waters), using a gradient of 5-36% B (buffer A 0.1% formic acid, buffer B 100% acetonitrile) over 16 minutes. Mass spectrometry experiments were performed on an Impact II TOF (Bruker) acquiring over a mass range from 150 to 2200 *m/z* using an electrospray ionization source operated at a temperature of 200 °C and a spray voltage of 4.5 kV. Peptides were identified using data-dependent acquisition methods following tandem MS/MS experiments (0.5 s precursor scan from 150-2000 *m/z*; twelve 0.25 s fragment scans from 150-2000 *m/z*). MS/MS datasets were analyzed using PEAKS7 (PEAKS), and a false discovery rate was set at 1% using a database of purified proteins and known contaminants.

HD-Examiner Software (Sierra Analytics) was used to automatically calculate the level of deuterium incorporation into each peptide. All peptides were manually inspected for correct charge state and presence of overlapping peptides. Deuteration levels were calculated using the centroid of the experimental isotope clusters. Results for these proteins are presented as relative levels of deuterium incorporation and the only control for back exchange was the level of deuterium present in the buffer (73.2% for experiments with pY; 74.2% for experiments without pY). The average error of all time points and conditions for each HDX project was 0.7% and 0.1 Da. Therefore, changes in any peptide at any time point greater than both 5% and 0.4 Da between conditions with a paired t-test value of *p* < 0.05 was considered significant. Full deuterium exchange information for all peptides analysed are shown in Fig. S1-S6.

## ACKNOWLEDGEMENTS

J.E.B. is supported by a new investigator grant from CIHR, and a discovery research grant from the Natural Sciences and Engineering Research Council of Canada (NSERC-2014-05218). We thank Thomas Buckles and Joseph Falke for assistance with the HRas coupling protocol.

## CONFLICT OF INTEREST

The authors declare no conflicts of interest

## AUTHOR CONTRIBUTIONS

B.D.S. and J.E.B. conceived and designed all biochemical experiments in the manuscript. All biochemical assays were performed by B.D.S. All HDX-MS experiments were designed and performed by J.E.B., M.K.R. and M.L.J. Data analysis was performed by B.D.S. M.K.R. M.L.J. and J.E.B. B.D.S. M.K.R. and J.E.B. wrote the manuscript. All authors approved the final version of the manuscript.

## REFERENCES

1. Balla, T. (2013) Phosphoinositides: tiny lipids with giant impact on cell regulation. *Physiol. Rev.* **93**, 1019–1137
2. Vanhaesebroeck, B., Stephens, L., and Hawkins, P. (2012) PI3K signalling: the path to discovery and understanding. *Nat. Rev. Mol. Cell Biol.* **13**, 195–203
3. Burke, J. E., and Williams, R. L. (2015) Synergy in activating class I PI3Ks. *Trends in Biochemical Sciences.* **40**, 88–100
4. Vadas, O., Burke, J. E., Zhang, X., Berndt, A., and Williams, R. L. (2011) Structural basis for activation and inhibition of class I phosphoinositide 3-kinases. *Sci Signal.* **4**, 1–13
5. Rodriguez-Viciana, P., Warne, P. H., Dhand, R., Vanhaesebroeck, B., Gout, I., Fry, M. J., Waterfield, M. D., and Downward, J. (1994) Phosphatidylinositol-3-OH kinase as a direct target of Ras. *Nature.* **370**, 527–532
6. Samuels, Y., Wang, Z., Bardelli, A., Silliman, N., Ptak, J., Szabo, S., Yan, H., Gazdar, A., Powell, S., Riggins, G., Willson, J., Markowitz, S., Kinzler, K., Vogelstein, B., and Velculescu, V. (2004) High frequency of mutations of the PIK3CA gene in human cancers. *Science.* **304**, 554
7. Angulo, I., Vadas, O., Garçon, F., Banham-Hall, E., Plagnol, V., Leahy, T. R., Baxendale, H., Coulter, T., Curtis, J., Wu, C., Blake-Palmer, K., Perisic, O., Smyth, D., Maes, M., Fiddler, C., Juss, J., Cilliers, D., Markelj, G., Chandra, A., Farmer, G., Kielkowska, A., Clark, J., Kracker, S., Debré, M., Picard, C., Pellier, I., Jabado, N., Morris, J. A., Barcenas-Morales, G., Fischer, A., Stephens, L., Hawkins, P., Barrett, J. C., Abinun, M., Clatworthy, M., Durandy, A., Doffinger, R., Chilvers, E. R., Cant, A. J., Kumararatne, D., Okkenhaug, K., Williams, R. L., Condliffe, A., and Nejentsev, S. (2013) Phosphoinositide 3-kinase  $\delta$  gene mutation predisposes to respiratory infection and airway damage. *Science.* **342**, 866–871
8. Ostrem, J. M. L., and Shokat, K. M. (2016) Direct small-molecule inhibitors of KRAS: from structural insights to mechanism-based design. *Nat Rev Drug Discov.* **15**, 771–785
9. Prior, I. A., Lewis, P. D., and Mattos, C. (2012) A Comprehensive Survey of Ras Mutations in Cancer. *Cancer Res.* **72**, 2457–2467
10. Geering, B., Cutillas, P., Nock, G., Gharbi, S., and Vanhaesebroeck, B. (2007) Class IA phosphoinositide 3-kinases are obligate p85-p110 heterodimers. *Proc. Natl. Acad. Sci. U.S.A.* **104**, 7809–7814
11. Knight, Z., Gonzalez, B., Feldman, M., Zunder, E., Goldenberg, D., Williams, O., Loewith, R., Stokoe, D., Balla, A., Toth, B., Balla, T., Weiss, W., Williams, R., and Shokat, K. (2006) A pharmacological map of the PI3-K family defines a role for p110 $\alpha$  in insulin signaling. *Cell.* **125**, 733–747
12. Fritsch, R., de Krijger, I., Fritsch, K., George, R., Reason, B., Kumar, M. S., Diefenbacher, M.,

- Stamp, G., and Downward, J. (2013) RAS and RHO families of GTPases directly regulate distinct phosphoinositide 3-kinase isoforms. *Cell*. **153**, 1050–1063
13. Dbouk, H. A., Vadas, O., Shymanets, A., Burke, J. E., Salamon, R. S., Khalil, B. D., Barrett, M. O., Waldo, G. L., Surve, C., Hsueh, C., Perisic, O., Harteneck, C., Shepherd, P. R., Harden, T. K., Smrcka, A. V., Taussig, R., Bresnick, A. R., Nürnberg, B., Williams, R. L., and Backer, J. M. (2012) G protein-coupled receptor-mediated activation of p110 $\beta$  by G $\beta\gamma$  is required for cellular transformation and invasiveness. *Sci Signal*. **5**, ra89
  14. Maier, U., Babich, A., and Nurnberg, B. (1999) Roles of non-catalytic subunits in gbetagamma-induced activation of class I phosphoinositide 3-kinase isoforms beta and gamma. *J. Biol. Chem*. **274**, 29311–29317
  15. Delgado, P., Cubelos, B., Calleja, E., Martínez-Martín, N., Ciprés, A., Mérida, I., Bellas, C., Bustelo, X. R., and Alarcón, B. (2009) Essential function for the GTPase TC21 in homeostatic antigen receptor signaling. *Nat. Immunol*. **10**, 880–888
  16. Pacold, M. E., Suire, S., Perisic, O., Lara-Gonzalez, S., Davis, C. T., Walker, E. H., Hawkins, P. T., Stephens, L., Eccleston, J. F., and Williams, R. L. (2000) Crystal structure and functional analysis of Ras binding to its effector phosphoinositide 3-kinase gamma. *Cell*. **103**, 931–943
  17. Gupta, S., Ramjaun, A., Haiko, P., Wang, Y., Warne, P., Nicke, B., Nye, E., Stamp, G., Alitalo, K., and Downward, J. (2008) Binding of ras to phosphoinositide 3-kinase p110alpha is required for ras-driven tumorigenesis in mice. *Cell*. **129**, 957–968
  18. Murillo, M. M., Zelenay, S., Nye, E., Castellano, E., Lassailly, F., Stamp, G., and Downward, J. (2014) RAS interaction with PI3K p110 $\alpha$  is required for tumor-induced angiogenesis. *J. Clin. Invest*. **124**, 3601–3611
  19. Castellano, E., Sheridan, C., Thin, M. Z., Nye, E., Spencer-Dene, B., Diefenbacher, M. E., Moore, C., Kumar, M. S., Murillo, M. M., Grönroos, E., Lassailly, F., Stamp, G., and Downward, J. (2013) Requirement for Interaction of PI3-Kinase p110 $\alpha$  with RAS in Lung Tumor Maintenance. *Cancer Cell*. **24**, 617–630
  20. Mazhab-Jafari, M. T., Marshall, C. B., Smith, M. J., Gasmi-Seabrook, G. M. C., Stathopoulos, P. B., Inagaki, F., Kay, L. E., Neel, B. G., and Ikura, M. (2015) Oncogenic and RASopathy-associated K-RAS mutations relieve membrane-dependent occlusion of the effector-binding site. *Proc. Natl. Acad. Sci. U.S.A.* **112**, 6625–6630
  21. Mazhab-Jafari, M. T., Marshall, C. B., Stathopoulos, P. B., Kobashigawa, Y., Stambolic, V., Kay, L. E., Inagaki, F., and Ikura, M. (2013) Membrane-dependent modulation of the mTOR activator Rheb: NMR observations of a GTPase tethered to a lipid-bilayer nanodisc. *J. Am. Chem. Soc.* **135**, 3367–3370
  22. Gureasko, J., Galush, W. J., Boykevisch, S., Sondermann, H., Bar-Sagi, D., Groves, J. T., and Kuriyan, J. (2008) Membrane-dependent signal integration by the Ras activator Son of sevenless. *Nature Structural & Molecular Biology*. **15**, 452–461
  23. Lin, W.-C., Iversen, L., Tu, H.-L., Rhodes, C., Christensen, S. M., Iwig, J. S., Hansen, S. D., Huang, W. Y. C., and Groves, J. T. (2014) H-Ras forms dimers on membrane surfaces via a protein-protein interface. *Proc. Natl. Acad. Sci. U.S.A.* **111**, 2996–3001
  24. Mott, H. R., Carpenter, J. W., and Campbell, S. L. (1997) Structural and functional analysis of a mutant Ras protein that is insensitive to nitric oxide activation. *Biochemistry*. **36**, 3640–3644
  25. Rodriguez-Viciana, P., Warne, P. H., Vanhaesebroeck, B., Waterfield, M. D., and Downward, J. (1996) Activation of phosphoinositide 3-kinase by interaction with Ras and by point mutation. *EMBO J.* **15**, 2442–2451
  26. Rodriguez-Viciana, P., Sabatier, C., and McCormick, F. (2004) Signaling specificity by Ras family GTPases is determined by the full spectrum of effectors they regulate. *Mol. Cell. Biol.* **24**, 4943–4954
  27. Masson, G. R., Perisic, O., Burke, J. E., and Williams, R. L. (2016) The intrinsically disordered tails of PTEN and PTEN-L have distinct roles in regulating substrate specificity and membrane activity. *Biochem. J.* **473**, 135–144

28. Vadas, O., and Burke, J. E. (2015) Probing the dynamic regulation of peripheral membrane proteins using hydrogen deuterium exchange-MS (HDX-MS). *Biochem. Soc. Trans.* **43**, 773–786
29. Burke, J. E., Perisic, O., Masson, G. R., Vadas, O., and Williams, R. L. (2012) Oncogenic mutations mimic and enhance dynamic events in the natural activation of phosphoinositide 3-kinase p110 $\alpha$  (PIK3CA). *Proc. Natl. Acad. Sci. U.S.A.* **109**, 15259–15264
30. Burke, J. E., Hsu, Y.-H., Deems, R. A., Li, S., Woods, V. L., and Dennis, E. A. (2008) A phospholipid substrate molecule residing in the membrane surface mediates opening of the lid region in group IVA cytosolic phospholipase A2. *J. Biol. Chem.* **283**, 31227–31236
31. Burke, J. E., Karbarz, M. J., Deems, R. A., Li, S., Woods, V. L., and Dennis, E. A. (2008) Interaction of group IA phospholipase A2 with metal ions and phospholipid vesicles probed with deuterium exchange mass spectrometry. *Biochemistry*. **47**, 6451–6459
32. Dornan, G. L., Siempelkamp, B. D., Jenkins, M. L., Vadas, O., Lucas, C. L., and Burke, J. E. (2017) Conformational disruption of PI3K $\delta$  regulation by immunodeficiency mutations in PIK3CD and PIK3R1. *Proc. Natl. Acad. Sci. U.S.A.* 10.1073/pnas.1617244114
33. Huang, C., Mandelker, D., Schmidt-Kittler, O., Samuels, Y., Velculescu, V., Kinzler, K., Vogelstein, B., Gabelli, S., and Amzel, L. (2007) The structure of a human p110 $\alpha$ /p85 $\alpha$  complex elucidates the effects of oncogenic PI3K $\alpha$  mutations. *Science*. **318**, 1744–1748
34. Park, M.-J., Sheng, R., Silkov, A., Jung, D.-J., Wang, Z.-G., Xin, Y., Kim, H., Thiagarajan-Rosenkranz, P., Song, S., Yoon, Y., Nam, W., Kim, I., Kim, E., Lee, D.-G., Chen, Y., Singaram, I., Wang, L., Jang, M. H., Hwang, C.-S., Honig, B., Ryu, S., Lorieau, J., Kim, Y.-M., and Cho, W. (2016) SH2 Domains Serve as Lipid-Binding Modules for pTyr-Signaling Proteins. *Mol. Cell*. **62**, 7–20
35. Burke, J. E., Vadas, O., Berndt, A., Finegan, T., Perisic, O., and Williams, R. L. (2011) Dynamics of the phosphoinositide 3-kinase p110 $\delta$  interaction with p85 $\alpha$  and membranes reveals aspects of regulation distinct from p110 $\alpha$ . *Structure*. **19**, 1127–1137
36. Suire, S., Hawkins, P., and Stephens, L. (2002) Activation of phosphoinositide 3-kinase gamma by Ras. *Curr. Biol.* **12**, 1068–1075
37. Vadas, O., Dbouk, H. A., Shymanets, A., Perisic, O., Burke, J. E., Abi Saab, W. F., Khalil, B. D., Harteneck, C., Bresnick, A. R., Nürnberg, B., Backer, J. M., and Williams, R. L. (2013) Molecular determinants of PI3K $\gamma$ -mediated activation downstream of G-protein-coupled receptors (GPCRs). *Proc. Natl. Acad. Sci. U.S.A.* **110**, 18862–18867
38. Welsch, M. E., Kaplan, A., Chambers, J. M., Stokes, M. E., Bos, P. H., Zask, A., Zhang, Y., Sanchez-Martin, M., Badgley, M. A., Huang, C. S., Tran, T. H., Akkiraju, H., Brown, L. M., Nandakumar, R., Cremers, S., Yang, W. S., Tong, L., Olive, K. P., Ferrando, A., and Stockwell, B. R. (2017) Multivalent Small-Molecule Pan-RAS Inhibitors. *Cell*. **168**, 878–889. e29
39. Vadas, O., Jenkins, M. L., Dornan, G. L., and Burke, J. E. (2017) Using Hydrogen-Deuterium Exchange Mass Spectrometry to Examine Protein-Membrane Interactions. *Meth. Enzymol.* **583**, 143–172

## FOOTNOTES

The abbreviations used are: PI3K, phosphoinositide 3-kinase; PIP<sub>3</sub>, phosphatidylinositol 3,4,5 trisphosphate; HDX-MS, Hydrogen deuterium exchange mass spectrometry; RTKs, Receptor Tyrosine Kinases; ABD, adaptor-binding domain; RBD, Ras-binding domain; PIP<sub>2</sub>, phosphatidylinositol 4,5 bisphosphate; PE-MCC, maleimidomethyl phosphoethanolamine; PC, phosphatidylcholine; PS, phosphatidylserine; PE, phosphatidylethanolamine; sHRas, soluble HRas; pY, phosphopeptide; GAP, GTPase-activating protein; GEF, guanine-nucleotide exchange factor



## FIGURES AND FIGURE LEGENDS

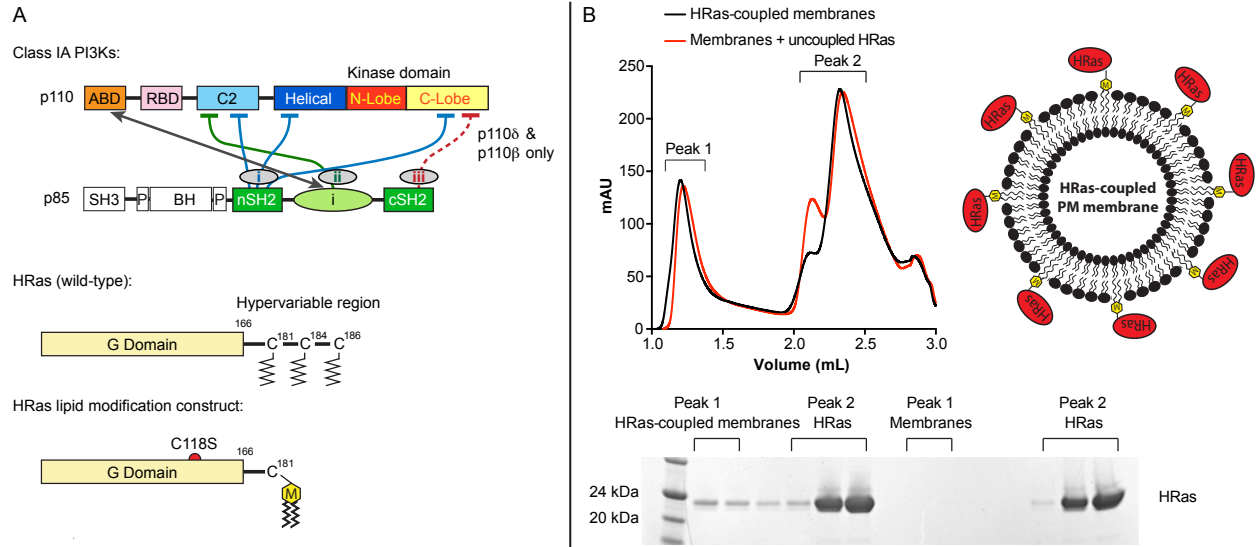


**Figure 1. Schematic of protein constructs and generation of HRas-coupled membranes. (A)** Domain architecture of class IA. Class IA PI3Ks are obligate heterodimers consisting of both a catalytic (p110) and regulatory (p85) subunits. The p110 subunit is composed of an adaptor-binding domain (ABD), Ras-binding domain (RBD), C2 domain, helical domain, and kinase domain. The p85 subunit is composed of a Src homology 3 domain (SH3), a Bar cluster region homology domain (BH), two proline-rich regions, and two Src homology 2 domains (nSH2 and cSH2) separated by a coiled-coil inter-SH2 domain (iSH2). The p110 and p85 subunits of PI3Ks interact via an iSH2-ABD interaction and the p85 subunit makes many important inhibitory contacts with p110 (i-iii). The cSH2-kinase domain inhibitory contact (iii) only occurs with p110 $\beta$  and p110 $\delta$  but not p110 $\alpha$ . HRas is composed of a G domain, which is involved in GTP binding, and a hypervariable region, which is subject to differential lipidation at three C-terminal cysteines. Our HRas lipid modification construct contains two substitution mutations (G12V, C118S) and ends at cysteine 181, which is subject to maleimide coupling. **(C)** Gel-filtration traces of HRas-coupled membranes and uncoupled HRas with membranes and associated SDS-PAGE of fractions. HRas-coupled membranes are clearly separated from uncoupled HRas. Gel filtration was carried out on a Superdex™ 200 5/150 GL Increase column (GE Healthcare).

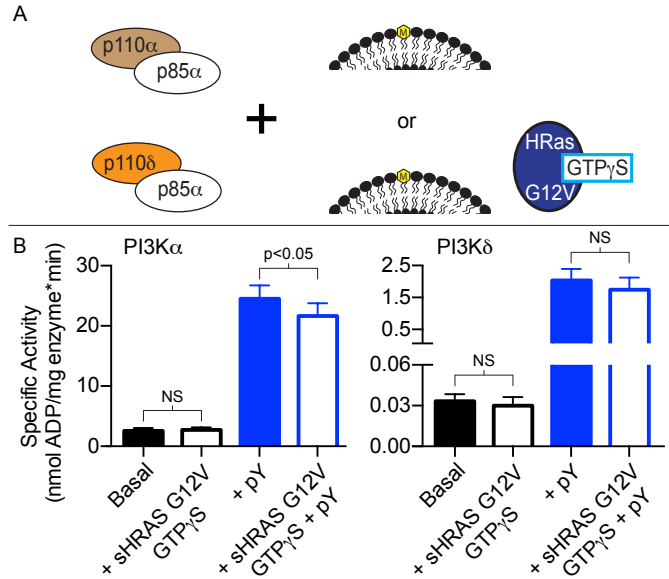


**Figure 2. PI3K $\alpha$  and PI3K $\delta$  are not activated by soluble HRas in a basal or phosphopeptide-stimulated state.** (A) Schematic of conditions tested in the kinase assays. PI3K $\alpha$  or PI3K $\delta$  was added to maleimide-quenched plasma membrane mimic vesicles in the presence or absence of soluble HRas (sHRas). (B) Specific activities of both PI3K $\alpha$  and PI3K $\delta$  in four different conditions: basal (vesicles only), in the presence of soluble HRas, RTK-derived phosphopeptide (1  $\mu$ M), or both soluble HRas and phosphopeptide. Assays measured the production of ADP in the presence of 1-1000 nM of PI3K, 100  $\mu$ M ATP, 0.45 mg/mL 5% PIP<sub>2</sub>/10% PE-MCC/15% PC/30% PS/40% PE vesicles, and 5  $\mu$ M soluble HRas. Kinase assays were performed in triplicate (representative assay; error shown as SD; n=3); p-values greater than 0.05 are shown as not significant (NS).

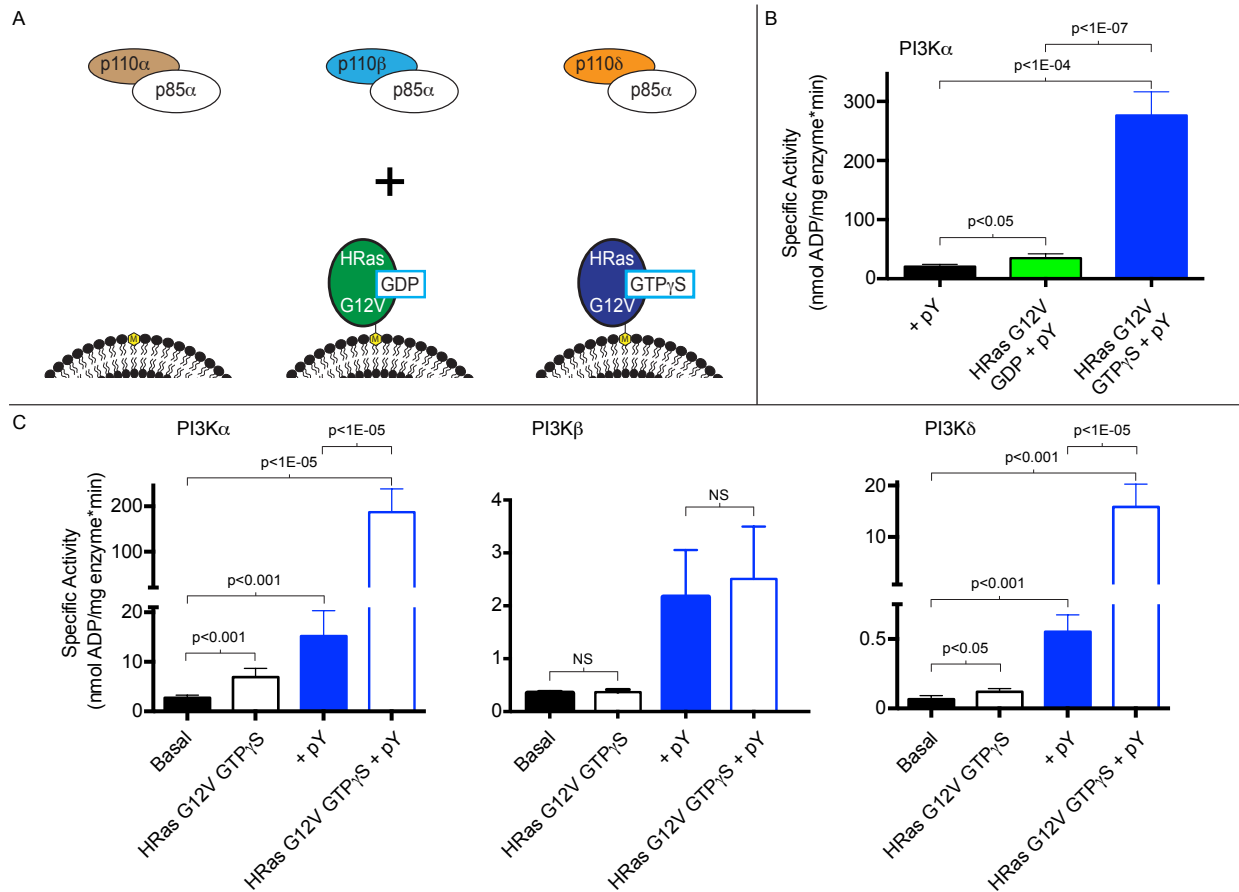


**Figure 3. PI3K $\alpha$  and PI3K $\delta$ , but not PI3K $\beta$ , are activated by HRas-coupled vesicles in a basal or phosphopeptide-stimulated state.** (A) Schematic of kinase assay conditions. PI3Ks were added to either HRas-coupled (GTP $\gamma$ S or GDP loaded) or uncoupled maleimide-functionalized plasma membrane mimic vesicles. (B) PI3K activation mediated by HRas-coupled vesicles is dependent on bound nucleotide. Specific activities of PI3K $\alpha$  in the presence of phosphopeptide in the presence or absence of HRas loaded with GDP or GTP $\gamma$ S. (C) Specific activities of both PI3K $\alpha$ , PI3K $\beta$ , and PI3K $\delta$  in four different conditions: basal (vesicles only), in the presence of GTP $\gamma$ S-loaded HRas-coupled vesicles, RTK-derived phosphopeptide, or both HRas-coupled vesicles and phosphopeptide. Assays measured the production of ADP in the presence of 1-1000 nM of PI3K, 100  $\mu$ M ATP, 0.45 mg/mL 5% PIP $_2$ /10% PE-MCC/15% PC/30% PS/40% PE vesicles, and 1.3  $\mu$ M membrane-bound HRas. Kinase assays were performed in triplicate (error shown as SD; n=3); p-values greater than 0.05 are shown as not significant (NS).

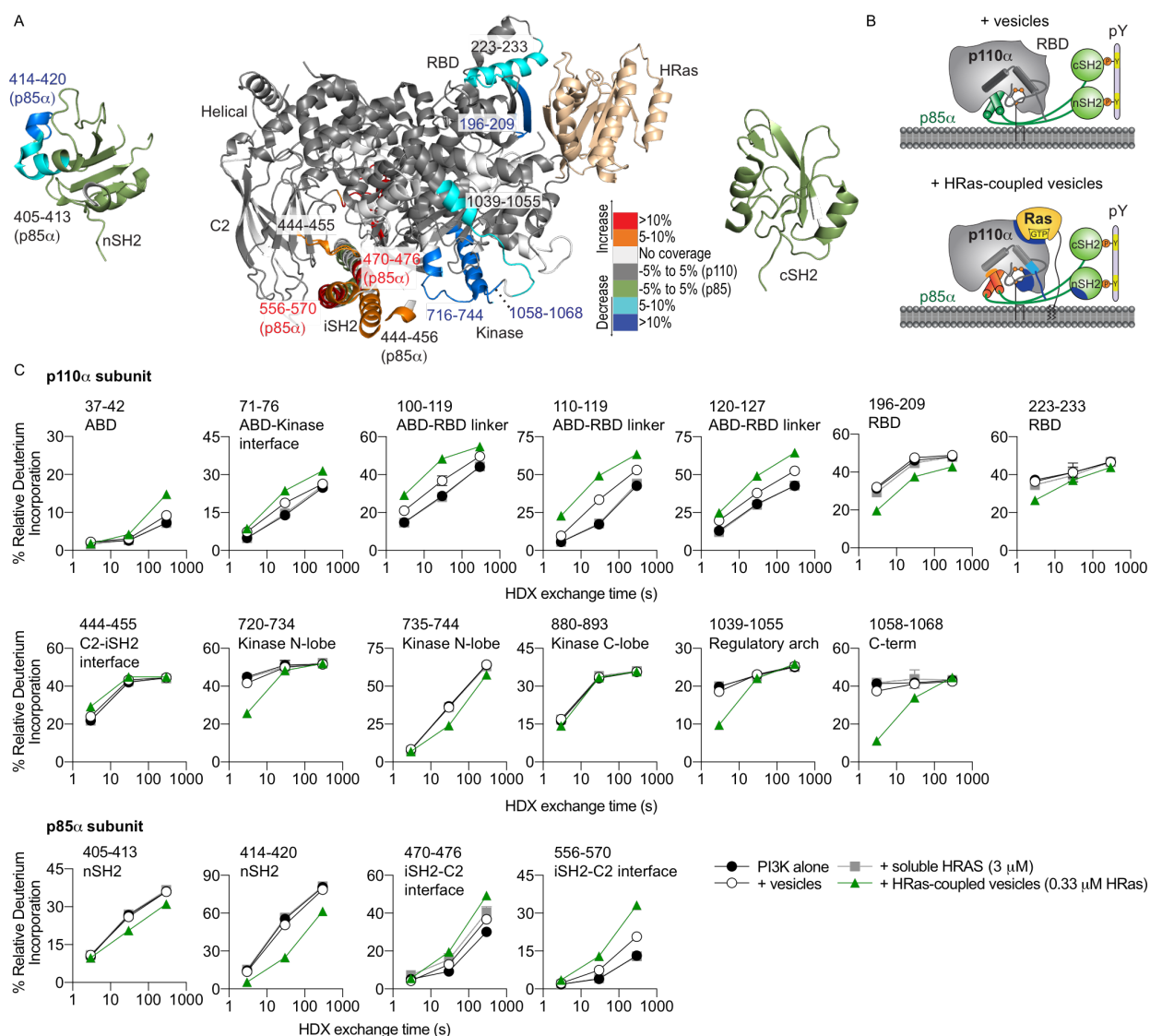


**Figure 4.** HDX-MS reveals the mechanism of PI3K $\alpha$  activation by membrane-coupled HRas. **(A)** Peptides in p110 $\alpha$  and p85 $\alpha$  which showed deuterium exchange differences greater than 5% and 0.4 Da between vesicles and HRas-coupled vesicles conditions are mapped on the modeled structure of PI3K $\alpha$  [PDB IDs: 3HHM (p110 $\alpha$ , nSH2-iSH2), 2Y3A (cSH2), and 1HE8 (HRas)]. The nSH2 is shown disconnected from p110 $\alpha$  to represent the phosphopeptide-bound state. **(B)** Schematic representations of PI3K $\alpha$  in its pY-activated state with mapped changes in deuterium exchange associated with HRas-coupled vesicles relative to the vesicles-only condition. **(C)** Time course of deuterium incorporation for peptides in both p110 $\alpha$  and p85 $\alpha$  showing differences in percent deuteration between the shown conditions (error shown as SD; n=3). Concentrations in parentheses refer to HRas, membrane was present at 0.2 mg/ml, and pY was present at 5  $\mu$ M.



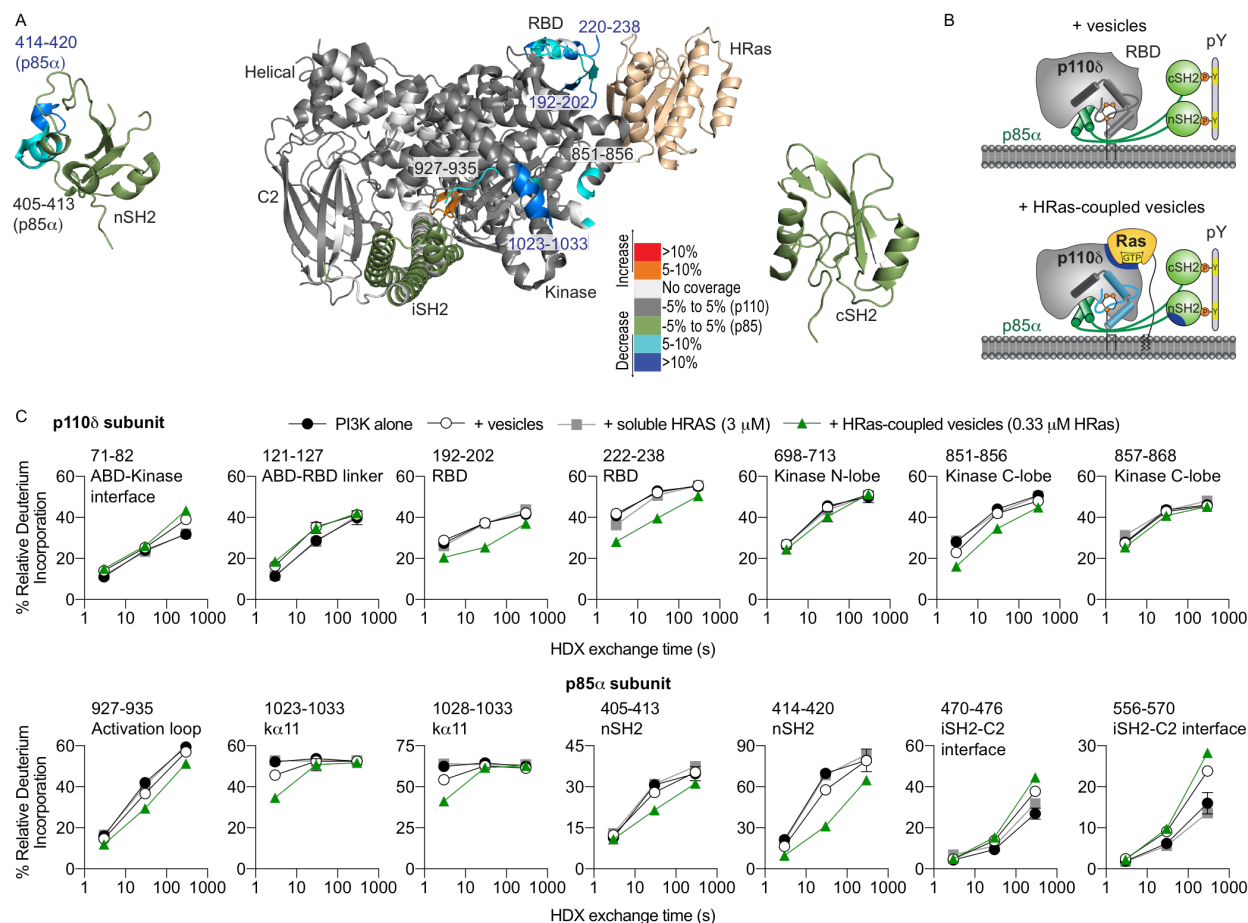


**Figure 5.** HDX-MS reveals the mechanism of PI3K $\delta$  activation by membrane-coupled HRas. **(A)** Peptides in p110 $\delta$  and p85 $\alpha$  which showed differences greater than 5% and 0.4 Da between vesicles and HRas-coupled vesicles conditions are mapped on the modeled structure of PI3K $\delta$  [PDB IDs: 5DXU (p110 $\delta$ , iSH2), 3HHM (nSH2), 2Y3A (cSH2) and 1HE8 (HRas)]. The nSH2 and cSH2 are shown disconnected from p110 $\delta$  to represent the phosphopeptide-bound state. **(B)** Schematic representations of PI3K $\delta$  in its pY-activated state with mapped changes in deuterium exchange associated with HRas-coupled vesicles relative to the vesicles-only condition. **(C)** Time course of deuterium incorporation for peptides in both p110 $\delta$  and p85 $\alpha$  showing differences in percent deuteration between the shown conditions (error shown as SD; n=3). Concentrations in parentheses refer to HRas, membrane was present at 0.2 mg/ml, and pY was present at 5  $\mu$ M.

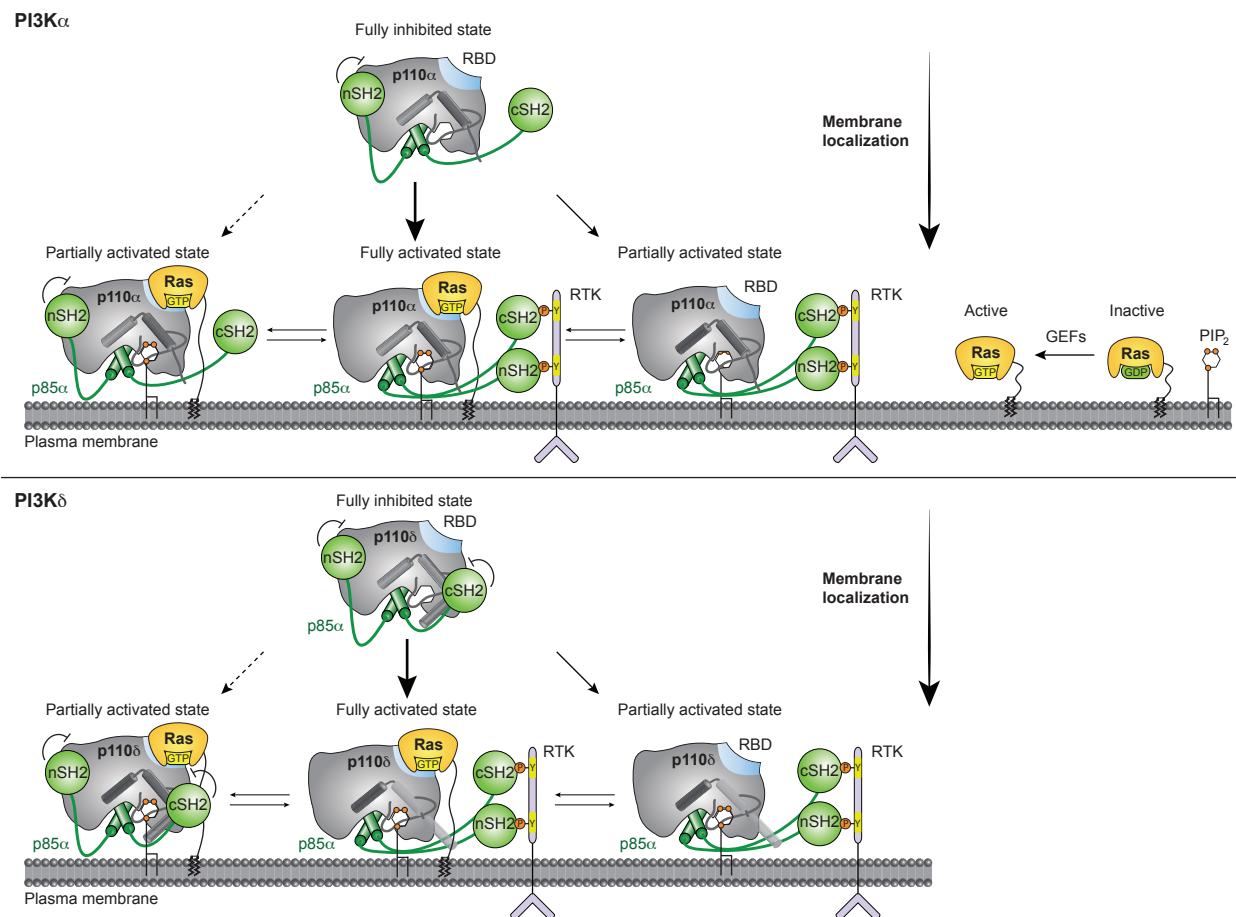


**Figure 6.** Depiction of PI3K $\alpha$  and PI3K $\delta$  activation by phosphorylated receptor-tyrosine kinases (RTKs) and Ras GTPases. Each individual input partially stimulates PI3K activity via membrane localization or the disruption of important inhibitory contacts, and all inputs are required for full activation. Ras proteins are activated by GEFs, which catalyze the exchange of GDP for GTP.

**Molecular mechanism of activation of class IA phosphoinositide 3-kinases (PI3Ks) by membrane-localized HRas**

Braden D Siempelkamp, Manoj K Rathinaswamy, Meredith L Jenkins and John E Burke

*J. Biol. Chem.* published online May 17, 2017

---

Access the most updated version of this article at doi: [10.1074/jbc.M117.789263](https://doi.org/10.1074/jbc.M117.789263)

Alerts:

- [When this article is cited](#)
- [When a correction for this article is posted](#)

[Click here](#) to choose from all of JBC's e-mail alerts

Supplemental material:

<http://www.jbc.org/content/suppl/2017/05/16/M117.789263.DC1>